Available online at www.sciencedirect.com
ScienceDirect
Earth and Planetary Science Letters 259 (2007) 107–118
EPSL
www.elsevier.com/locate/epsl

Magnetic proxy for the deep (Pacific) western boundary current variability across the mid-Pleistocene climate transition

Alessandra Venuti [a,b,*], Fabio Florindo [a], Elisabeth Michel [c], Ian R. Hall [d]

[a] Istituto Nazionale di Geofisica e Vulcanologia, Via di Vigna Murata 605, 00143, Roma, Italy
[b] Università degli Studi di Siena, Via del Laterino 8, 53100, Siena, Italy
[c] Laboratoire des Sciences du Climat et de l'Environnement, Avenue de la Terrasse, F-91198, Gif-sur-Yvette Cedex, France
[d] School of Earth, Ocean and Planetary Sciences, Cardiff University, PO Box 914, Cardiff CF10 3YE, UK

Received 27 September 2006; received in revised form 23 April 2007; accepted 23 April 2007
Available online 27 April 2007
Editor: M.L. Delaney

Abstract

The Deep Western Boundary Current (DWBC) inflow to the SW Pacific is one of the largest, transporting ~40% of the total input of deep water to the world's oceans. Here we use a sedimentary record from the giant piston core MD97-2114 collected on the northern flank of the Chatham Rise located at 1935 m water depth, east of New Zealand, to investigate DWBC variability during the Pleistocene epoch when the period of glacial cycles changed progressively from a 41 kyr to 100 kyr rhythm. Magnetic grain-size may be directly related to orbitally forced fluctuations in the strength of the upper circumpolar deep water (UCDW) through its interaction with terrigenous sediments supplied from the south and west. The long-term trends in magnetic properties are characterized by two main perturbations centered at 870 ka (Marine Isotope Stage, MIS 22) 450 ka (MIS 12), which is broadly consistent with the inferred perturbation during the mid-Pleistocene climate transition based on sedimentological paleocurrent reconstruction from Ocean Drilling Program Site 1123 located at 3290 m water depth in the main core of the DWBC flow on the North Chatham Drift. This similarity suggests that both the upper and middle CDW are modulated by similar processes and fluctuations of Antarctic Bottom Water production could be directly responsible for this deep Pacific Ocean inflow variability over the past 1.2 Ma.

Keywords: DWBC; Chatham Rise; New Zealand; Pleistocene; magnetostratigraphy; environmental magnetism

1. Introduction

The sedimentary system off the eastern margin of New Zealand (Eastern New Zealand Oceanic Sedimentary System) (e.g., Carter et al., 1996, 2004a), extending from the Solander Channel north to the Kermadec Trench (Fig. 1), is considered a key area to study the interactions between the largely wind-driven Antarctic Circumpolar Current (ACC) and the west Pacific Ocean circulation. Today, the supply of deep water to the South Pacific Ocean is dominated by the thermohaline Deep Western Boundary Current (DWBC) east of New Zealand, which was established since at least the latest Oligocene (Carter et al., 1996, 2004a). In terms of flux, with an average volume transport of 16±11.9 Sverdrups (1 Sv = 10^6 m^3 s^{-1}) at 32°30′S, this is one of the largest DWBC in the world ocean (Whitworth et al., 1999).

* Corresponding author. Istituto Nazionale di Geofisica e Vulcanologia, Via di Vigna Murata 605, 00143, Roma, Italy.
E-mail address: venuti@ingv.it (A. Venuti).

0012-821X/$ - see front matter © 2007 Published by Elsevier B.V.
doi:10.1016/j.epsl.2007.04.032

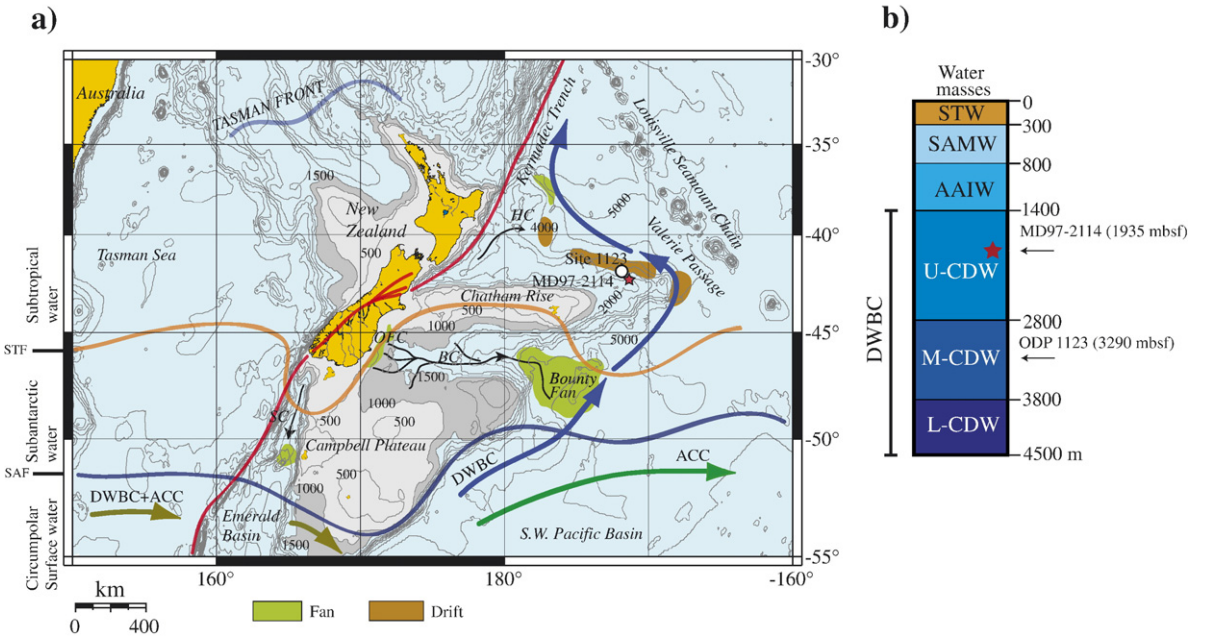

Fig. 1. (a) Site MD97-2114 is east of New Zealand. Shown are the average present-day positions of the major modern oceanographic fronts (STF, Subtropical Front; SAF, Subantarctic Front), the pathway of the Deep Western Boundary Current (DWBC) and the Antarctic Circumpolar Current (ACC) (after Carter et al., 1996, 2004a). Sediment is supplied down the Solander (SC), Bounty (BC) and Hikurangi (HC) channels to abyssal depths and into the path of the DWBC, which transports the material along the margin of the Chatham Rise/Hikurangi Plateau, depositing sediment drifts where the flow slows down. OFC = Otago Fan Complex. Bounty Fan and channel details are from Carter and Carter (1996). Location of ODP Site 1123 is indicated by a red star. (b) Water column subdivision. Shown are the water depth positions of site MD97-2114 and ODP Site 1123. STW = Subtropical water, SAMW = Sub-Antarctic Mode Water, and AAIW = Antarctic Intermediate Water.

The DWBC, in concert with the deep-reaching ACC, flows northeastward along the eastern edge of the Campbell Plateau until about 50°S latitude. Here, the DWBC and ACC decouple, with the ACC turning eastward, continuing its journey around Antarctica, and the DWBC passing the entrance to Bounty Channel, and then beneath the productive surface waters associated with the Subtropical Front (Fig. 1) (Murphy et al., 2001). The DWBC intensifies as it veers around the eastern tip of the Chatham Rise, being constrained by the steep sides (Carter and McCave, 1994; McCave and Carter, 1997; Warren, 1981), and then decelerates after passing through Valerie Passage, which separates the Chatham Rise from the NW–SE trending Louisville Seamount Chain (Hall et al., 2003).

The DWBC principally transports Circumpolar Deep Water (CDW) containing three major components (Fig. 1b) (McCave and Carter, 1997; Warren, 1973, 1981; Whitworth et al., 1999): (i) Upper CDW, a strongly nutrient-enriched and oxygen-depleted layer located between 1400 and 2800 m water depth, (ii) middle CDW, a distinct higher salinity (S = 34.72-34.73 practical salinity units, PSU) layer between 2800 and 3800 m, including the zone of maximum influence of North Atlantic Deep Water (2800 and 3400 m), and (iii) lower CDW, a cold and lower salinity (S = 34.68 PSU) layer >3800 m water depth. The latter waters are largely generated around Antarctica, in particular within the Weddell Sea, Ross Sea, and along the Adelie Coast (Rintoul et al., 2001) (i.e., *sensu lato* Antarctic Bottom Water). Hall et al. (2001) using sedimentological and geochemical paleohydrographic proxies from Ocean Drilling Program (ODP) Site 1123 (3290 m water depth), reported evidence for intensified DWBC inflow and Pacific Ocean ventilation during glacial periods over the past 1.2 Ma. This is believed to be directly related to increased glacial production of Antarctic Bottom Water. This time series records the middle CDW component of the DWBC flow, mainly derived from Indian Ocean outflow added to Pacific outflow returning through the Drake Passage. Three longer-term periods of differing mean flow speeds are identified within the past 1.2 Ma, with the interval related to the mid-Pleistocene climate transition between 870–450 ka the period of change in the dominant response of the Earth's climate from orbital obliquity to eccentricity forcing (e.g., EPICA Community Members, 2004; Schmieder et al., 2000) characterized by generally weaker DWBC flow.

Here we present marine sediment records of magnetic properties and planktonic foraminifera $\delta^{18}O$

isotope measurements from a middle/upper Pleistocene depositional sequence from the northern flank of the Chatham Rise, east of New Zealand (Fig. 1). The site is well placed to monitor the variability of the upper CDW component of the deep Pacific inflow. This study examines whether (1) the "mid-Pleistocene climate transition" in ice volume and its frequency of variation was associated with changes in the upper DWBC circulation, and (2) whether these changes are recorded by sedimentary magnetic properties.

2. Site location and the MD97-2114 sediment core

The 28-m-long Calypso giant piston core (GPC) MD97-2114 was recovered in May 1997 during the IMAGES III cruise of the R/V *Marion-Dufresne*, and was part of a south to north transect from New Zealand to China Sea. The core site is located in the northeastern flank of the Chatham Rise (42°22′27″S, 171°20′42″W), east of New Zealand, north of the present-day Subtropical Front. At a water depth of 1935 m, the seafloor at this site is presently influenced by upper CDW (Fig. 1). The sedimentary sequence is dominated by light gray to olive gray homogeneous mud with abundant calcareous nannoplankton and foraminifera (Cobianchi personal communication, 2006). The site is presently above the carbonate compensation depth, which is regionally located at about 4400 m (McCave and Carter, 1997). The core contains several macroscopic rhyolitic tephra layers, which are well documented off eastern New Zealand, and are attributable to eruptions from the Taupo and Coromandel Volcanic zones, of central North Island (e.g., Carter et al., 2004b). Additional tephra layers are highlighted by peaks in the remanent magnetizations (see below).

3. Methods

3.1. Paleomagnetism

Low-field magnetic susceptibility measurements (κ) of core MD97-2114 were undertaken on the whole cores onboard the *RV Marion Dufresne* at 2 cm intervals, using a GEOTEK Multi Sensor Track equipped with a Bartington MS2C magnetic susceptibility meter. The split working halves were subsequently sub-sampled at the Core Repository of the Laboratoire des Sciences du Climat et de l'Environnement (LSCE), Gif-sur-Yvette, France, using standard u-channels for detailed paleomagnetic analyses.

All paleomagnetic measurements were made in the magnetically shielded paleomagnetic laboratory at the Istituto Nazionale di Geofisica e Vulcanologia (INGV), Rome, using a narrow-access pass-through cryogenic magnetometer (2-G Enterprises model 755R) with internal diameter of 4.2 cm, equipped with three DC SQUID sensors (noise level 3×10^{-9} A m^2 kg^{-1}). The natural remanent magnetization (NRM) was measured at 1-cm intervals, although smoothing occurs due to the Gaussian shape of the response curve of the magnetometer pick-up coils. The half-power width suggests smoothing across 4.8 cm for the radial x and y directions and 5.9 cm for the axial z direction (Weeks et al., 1993). Data from the upper and lower 6 cm of each u-channel were therefore discarded as they were affected by 'end effects' caused by the width of the magnetometer response function.

The NRM was alternating field (AF) demagnetized in eight steps, 10, 20, 30, 40, 50, 60, 80, and 100 mT, and measured after each step in order to define a magnetic polarity zonation. The characteristic remanent magnetization (ChRMs) inclinations were used to determine polarity, where negative inclinations indicate normal polarity intervals and positive inclinations indicate reversed polarity intervals in the Southern Hemisphere. Data from the 20–30 mT steps were used to estimate the ChRM direction for a large portion of the analyzed sediments.

After measurements and stepwise AF demagnetization of the NRM, a range of rock magnetic measurements were carried out on the same u-channels samples and chips (<50 mg) in order to examine the fluctuations in concentration, grain-size and composition of the magnetic fraction. Anhysteretic remanent magnetization (ARM) was imparted using a direct current (DC) bias field of 0.05 mT superimposed on a 100 mT peak AF, which was gradually reduced to zero. Isothermal remanent magnetization (IRM) was applied using DC bias field of 0.9 T and back-fields of 0.1 and 0.3 T. Hysteresis parameters were measured in a 0.5-T peak field on chip samples collected from the u-channels and distributed along the sequence using an alternating gradient magnetometer (AGM) (Princeton Measurements Corp. Model 2900 Micromag™). Backfield demagnetization of IRM was used to determine the coercivity of remanence (Bcr). The ratios of saturation remanence to saturation magnetization (Mrs/Ms) and coercivity of remanence to coercive force (Bcr/Bc) are useful indicators of the size of magnetic grains, as outlined by Day et al. (1977). However, it is worth noting that the extremely low magnetic grain concentrations hampered the study of hysteresis parameters and coercivity of remanence on a high number of samples. For discriminating ferromagnetic mineralogy, the temperature dependence

of the magnetic susceptibility, up to maximum temperature of 700 °C, was measured with a furnace equipped KLY-3 (AGICO) Kappabridge (noise level 2×10^{-8} SI). For a few selected samples, we also carried out a stepwise (at 120, 200, 250, 300, 350, 400, 450, 500, 550, 600, and 650 °C steps) thermal demagnetization of an IRM imparted in a 2.5 T field using a 2G Enterprises pulse magnetizer model 660.

3.2. Stable isotope data

Core MD97-2114 was sampled at 15 cm intervals to analyze stable isotopes at the LSCE. The planktonic foraminifer, *Globigerina bulloides*, was picked in the 250–315 μm size fraction and cleaned in an ultrasonic bath with methanol. Four to five specimens were used to measure the oxygen stable isotopic composition using a ThermoFinnigan Delta Plus mass spectrometer. All values are reported relative to VPDB, with measured values for $\delta^{18}O$ of −2.20‰ and −23.15‰ for NBS 19 and NBS 18 AIEA international standards, respectively. For this study, 26 random replicate analyses of a *Globigerina bulloides* sample from MD97-2114 gave a $\delta^{18}O$ reproducibility of 0.14‰ (1σ).

3.3. Spectral analysis

We used Analyseries 2.03 software package (Paillard et al., 1996) to detect the presence of harmonic components in the time series. The linear detrended data were processed using the Blackman–Tukey (BT) spectrum algorithm (Blackman and Tukey, 1958) and the Maximum Entropy (ME) technique (Press et al., 1993) (not shown here). The data series were tapered with a Bartlett-Window to reduce spectral leakage (Weedon, 2003). Using these techniques in combination allows a robust evaluation of the most significant spectral features and therefore ensured a high degree of confidence when interpreting the results.

4. Results and discussion

4.1. Age model

The age model for MD97-2114 core is based on a high-resolution magnetostratigraphy, integrated with $\delta^{18}O$ isotope measurements of *G. bulloides*. Our age assignment is further supported by preliminary quantitative analyses of calcareous nannofossil and planktonic foraminiferal assemblages which corroborate our age model (Cobianchi et al., 2005; Cobianchi personal communication, 2006).

The NRM intensity is generally low throughout the core, with a series of narrow peaks due to the presence of thin silicic tephra beds (e.g., Carter et al., 2004b). The presence of tephra beds is also well documented by the light reflectance profile (see Fig. 5). It is worth noting that a few NRM spikes are unaccompanied by even thin macroscopic tephra and this could be related to bioturbation processes that mixed the original tephra into the sediment (Kennett, 1981). A similar signal was also reported after a paleomagnetic investigation from the nearby Site 1123 located about 100 km north of site MD97-2114 (Fig. 1) (Shipboard Scientific Party, 1991). These weak intensities of magnetization are certainly responsible for the "noisy" characteristic remanent magnetization (ChRM) inclination record but this did not hamper the construction of a magnetic polarity zonation for this core (Figs. 2 and 3).

When compared with the reference geomagnetic polarity time scale (GPTS) (Cande and Kent, 1995), the Brunhes Chron (C1n; 0–0.78 Ma) is interpreted to be present from 0 to 19.70 m below seafloor (mbsf). The C1r.1r/C1r.1n reversal boundary (0.99 Ma) is present at 25.22 mbsf. The lower part of the core represents the upper part of the Jaramillo Subchron (C1r.1n). Using the Brunhes/Matuyama (B/M) and the upper Jaramillo reversal boundaries as age control points we matched the *G. bulloides* $\delta^{18}O$ record to the $\delta^{18}O$ stacked curve (LR04 stack) of Lisiecki and Raymo (2005) (Fig. 4). The isotope stack well agrees with other previously published stacks for the late Pleistocene and to the SPECMAP time scale back to 625 ka.

The reliability of the obtained time scale is supported by the identification of the same Milankovitch periodicities in the "tuned" *G. bulloides* $\delta^{18}O$ record (Fig. 4). This chronology implies an age of 1.06 Ma for the bottom of the sequence and an average sediment accumulation rate of ~2.6 cm/kyr.

4.2. Magnetic properties

Thermomagnetic experiments and relatively low coercivities imply that magnetite (and/or low Ti content titanomagnetite) is the primary remanence carrier. There is no evidence of antiferromagnetic minerals (i.e., hematite or goethite). Throughout the sequence magnetic susceptibility values are very low (Fig. 5a), which hampered attempts to measure the frequency dependence of susceptibility. Down-core variations of the NRM intensity are associated with similar changes in the ARM and IRM concentration-dependent parameters (Fig. 5b–d). The weak magnetic signal throughout this sedimentary record is associated with low concentrations of magnetic grains, particularly in the interval between ca. 10.50 and 18.50 mbsf. Low concentrations are expected

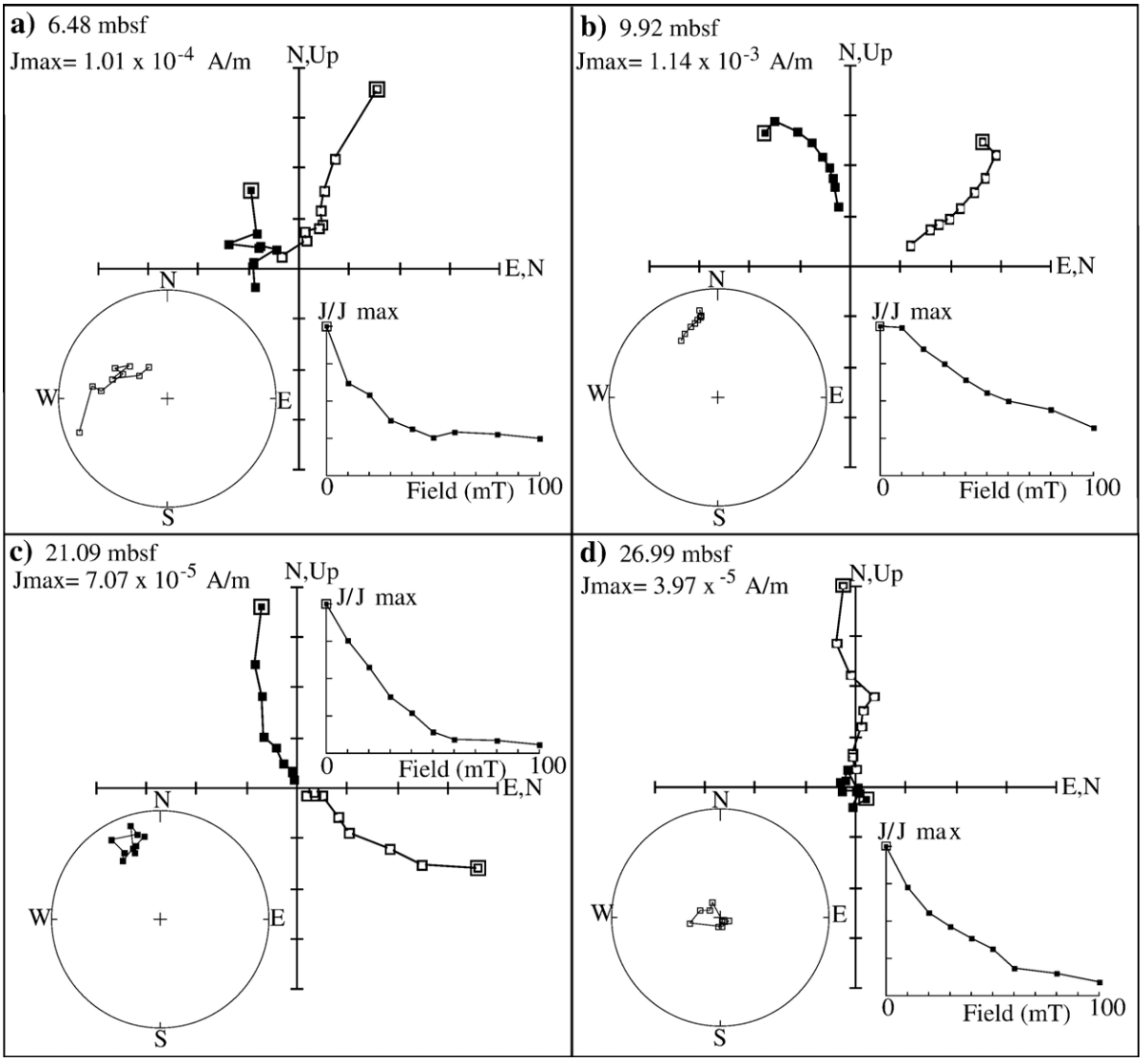

Fig. 2. (a–d) Typical AF demagnetization diagrams. Open and closed symbols represent the projection of the vector end-point onto the vertical and horizontal planes, respectively. (b) A more stable demagnetization behavior is evident in correspondence of a tephra layer.

when the terrigenous material was supplied from the South Island hinterland (Southern Alps), through the Bounty Fan system to MD97-2114. Sediment from this region is often depleted in magnetite through post-depositional diagenetic dissolution that occurred in marine sediments of the Torlesse Supergroup (e.g., Smale, 1990) and Neogene cover sequences before they were tectonically uplifted above sea level (e.g., Roberts and Turner, 1993; Rowan and Roberts, 2006).

For most of the analyzed samples, because the magnetic susceptibility is so weak its signal results in noisy susceptibility versus temperatures curves, which precludes the unequivocal determination of the Curie temperature. Only a few samples show a clear decrease in susceptibility near 580 °C which indicates the presence of magnetite. Susceptibilities are far higher for the cooling curves compared to the heating curves indicating that new magnetic phases (magnetite) were created during heating. The thermal demagnetization of the IRM confirms the presence of magnetite in these sediments. The intensities decrease in a quasi-linear fashion from room temperature to 580 °C, with only weak (if present) changes in the slope of the curve at ca 250 °C (Fig. 6).

The remanence and the coercivity ratios of these samples can be interpreted mostly as magnetites of pseudo single domain size (PSD; $0.5 < d < 10$ μm for

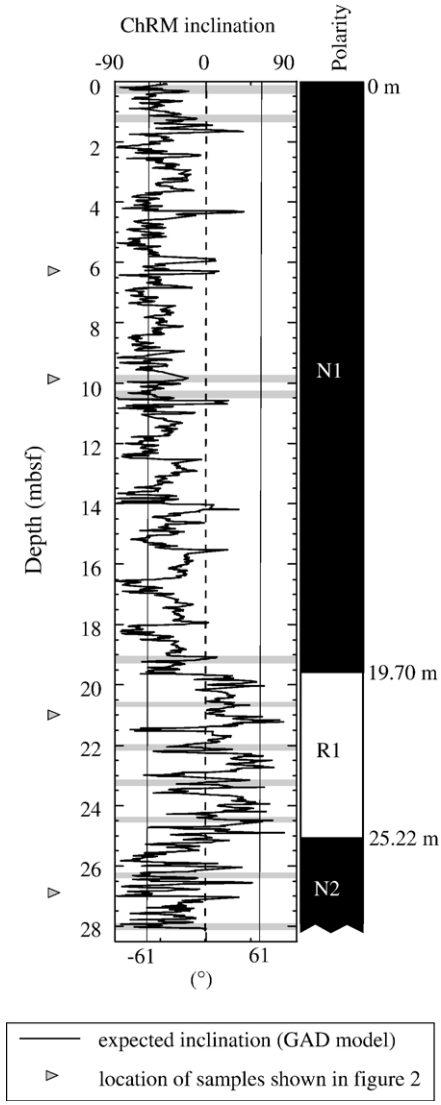

Fig. 3. $NRM_{20\ mT}$ inclination and polarity interpretation. Negative (positive) inclinations indicate normal (reversed) polarity.

magnetite). Only one sample, near the bottom of the sequence (sample MD 18–55 at 25.55 mbsf: Mr/Ms = 0.1; Hcr/Hc = 6.6), deviates from the standard PSD values, possibly indicating a mixture of PSD and SP (<0.03 μm) grains (Dunlop, 2002a,b) (Fig. 7). At this site we have no evidence of abundant SD bacterial magnetite, as found by Lean and McCave (1998) at the deeper core CHAT 1 K (41°35′S, 171°30′W, 3556 m water depth) and attributed to magnetotactic bacteria activity (Hesse, 1994; Moskowitz et al., 1993). We suggest here that different environmental conditions (e.g., changes in pore water oxygenation, availability of organic matter) did not favor the *in situ* growth of bacterial magnetite at this shallower site.

With the magnetic mineralogy constrained as magnetite, the ARM/IRM ratio is commonly used as an indicator of the quantity of fine (~0.1–1.0 μm diameter single domain and pseudo single domain) grains (e.g., Meynadier et al., 1995; Rousse et al., 2006; Shipboard Scientific Party, 2001), because the ARM is more effective in activating finer magnetite grains than the IRM. Therefore, abundant small (large) particles lead to higher (lower) values of the ratio. The down core record of this ratio shows distinctive short- and long-term trends, which are possibly connected to the dynamics of DWBC circulation (see below).

4.3. Magnetic properties and DWBC variability

Analogous to other commonly used magnetic grain-size parameters, the ARM/IRM ratio has been taken as a proxy for near-bottom current flow speed, where lower ratios reflect larger grains, and therefore stronger near-bottom flow, and vice versa (e.g., Snowball and Moros, 2003). However, as highlighted recently by McCave and Hall (2006) this interpretation of the ARM/IRM ratio is difficult to imagine as it implies a hydrodynamic sorting process for submicron sized grains that have to be deposited in aggregates. We suggest that the ARM/IRM ratio in core MD97-2114 most likely reflects a process of varying sediment supply driven by differential erosion and transport/deposition in the upstream DWBC, comparable to the resuspension and transport of magnetite by Iceland Scotland Overflow Waters around the Greenland–Scotland Ridge (Kissel, 2005). If this is the case, then the ARM/IRM ratio at MD97-2114 plausibly provides qualitative information on the changing dynamics of the UCDW component of the shallowest DWBC.

North of the Bounty Fan, along the path of the DWBC, the sedimentary terrigenous flux largely reflects the erosion and transport capacity of the DWBC (Hall et al., 2002). Because the Bounty Fan system discharges at depths exceeding 4000 m it may not be the main source of terrigenous sediment to MD97-2114 at 1935 m, a point brought out by Hall et al. (2002). At least three additional sources should be considered including: (1) the terrigenous material is possibly eroded from the upper flanks of Campbell Plateau by the ACC and transported north; (2) hemipelagic load generated in the head of Bounty Channel, especially during glacials, is transported east along the southern flank of Chatham Rise and then on to MD97-2114 (see Fig. 2 in Morris et al., 2001, which summarizes subsurface float trajectories); (3) sediment transported from the west along the northern flank of Chatham Rise via the East Cape Current which is known to move Northern New Zealand

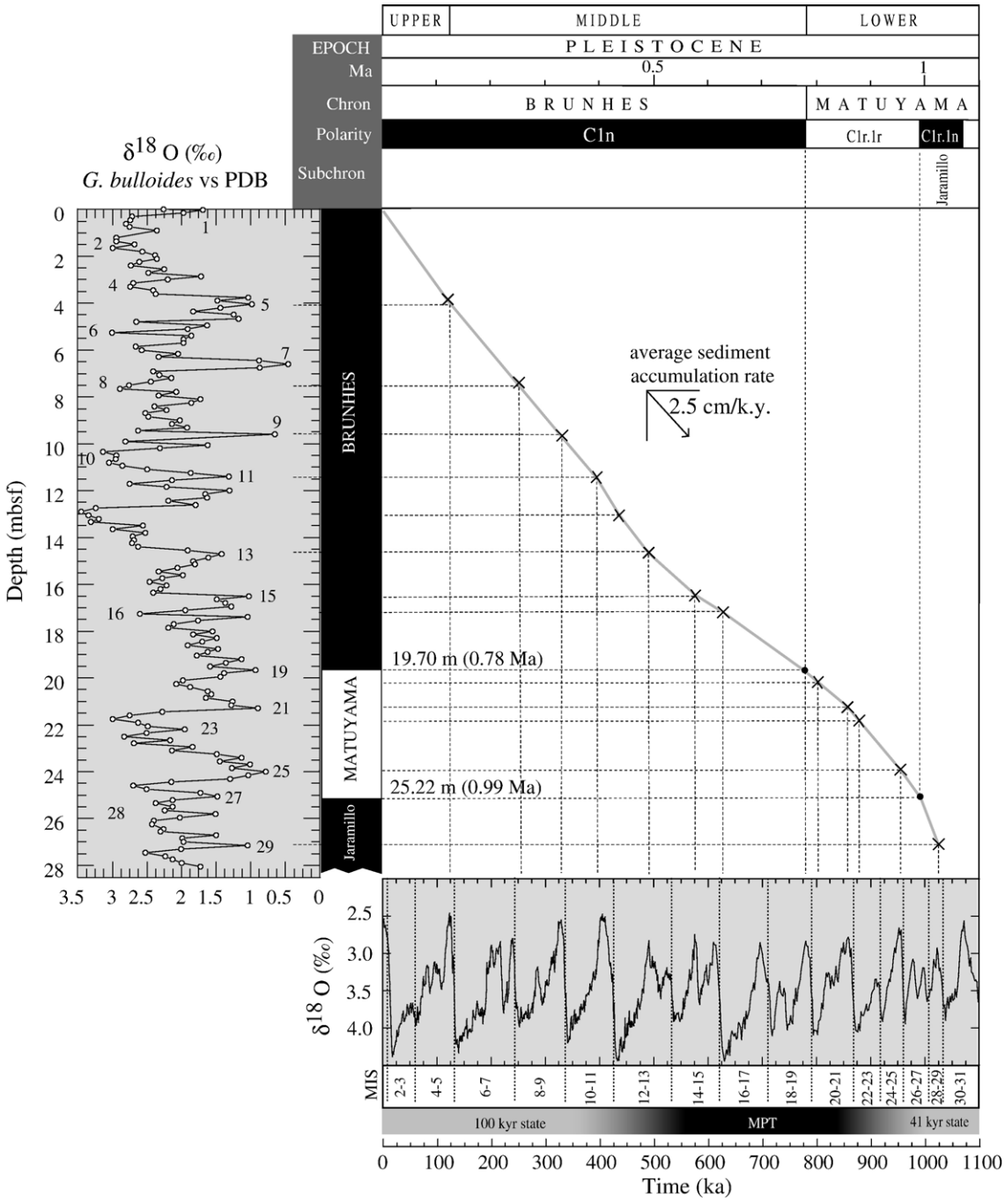

Fig. 4. Age versus depth plot of Site MD97-2114. Correlation of the magnetic polarity zonation and stable planktonic oxygen isotopic record with the geomagnetic polarity time scale (GPTS) of Cande and Kent (1995) and to the global benthic stack curve of Lisiecki and Raymo (2005). Glacial and interglacial periods are numbered following the terminology of SPECMAP (Shackleton et al., 1990 and references therein). The correlation between our $\delta^{18}O$ curve and the global stack of Lisiecki and Raymo (2005) is further supported by preliminary quantitative analyses of calcareous nannofossil and planktonic foraminiferal assemblages (Cobianchi et al., 2005; Cobianchi personal communication, 2006) and by two further tie points provided by the Brunhes/Matuyama (MIS=19) and the upper Jaramillo (MIS=27) reversal boundaries. MPT=mid-Pleistocene transition.

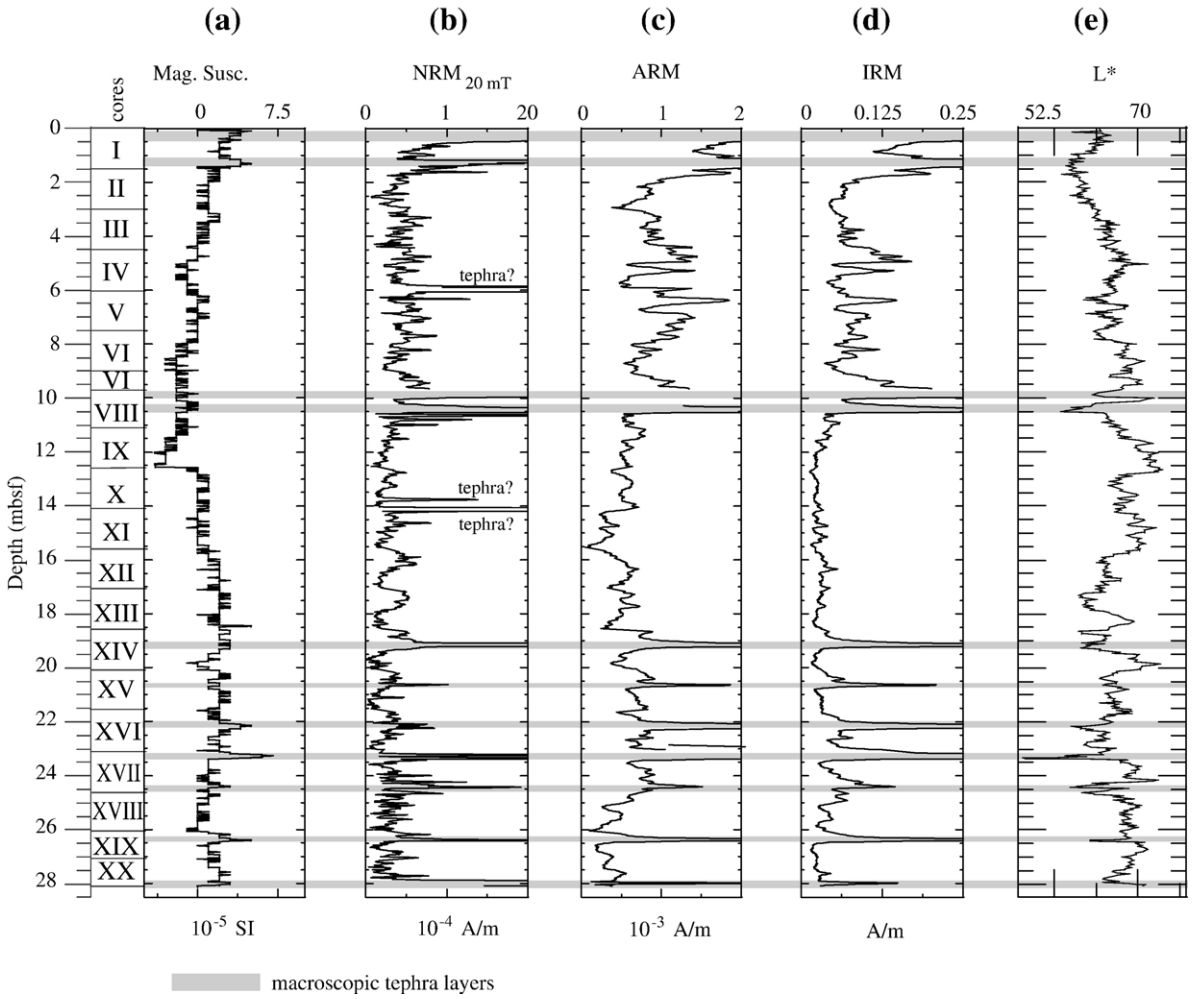

Fig. 5. Paleomagnetic data for core MD97-2114. (a) The u-channel magnetic susceptibility data, (b) $NRM_{20\ mT}$ intensity, (c) ARM intensity, and (d) IRM intensity. (e) The light reflectance profile, measured from sediment cores split onboard using the Minolta CM-2002 handheld spectrophotometer, is shown on the log to the right. Grey bars mark the position of rhyolitic tephra layers.

sediment to Site 1123 as indicated by pollen tracers (Mildenhall et al., 2004). Blackman–Tukey spectral analysis (Blackman and Tukey, 1958) of the oxygen isotopes record (Fig. 8b) shows significant (at 90% level) power at the eccentricity and obliquity orbital frequencies.

The ARM/IRM record although complicated by the presence of tephra layers that render the record noisy, also shows significant (at 90% level) power at these orbital frequencies and also precession (Fig. 8b). These findings provide likely evidence for an external forcing mechanism that drives the strength and water-mass properties of the upper DWBC during the early–middle Pleistocene transition.

The ARM/IRM data series (Fig. 8a) also show distinctive long-term trends, which again most likely reflect secular changes in the strength of the upper DWBC circulation: relatively low ARM/IRM ratios (relatively strong flow strength) occurred over the last 300 kyr and before ca. 870 ka. A major event, marked by an ARM/IRM increase (relatively weaker flow strength), occurs at ca. 450 ka (Marine isotope stage, MIS 12). Another is recognizable at ca. 870 ka (MIS 22). These observations are broadly consistent with the suggestion of a significant perturbation during the mid-Pleistocene climate transition between 860 and 450 ka reported from grain-size based paleocurrent analyses of sediment material recovered at ODP Site 1123 under the influence of the middle CDW (Hall et al., 2001). Such similarity between our records and the dynamic and the paleohydrographic reconstructions from Site 1123 suggests a regional character of these deep-water events. However, a significant difference between our ARM/IRM record and the Site

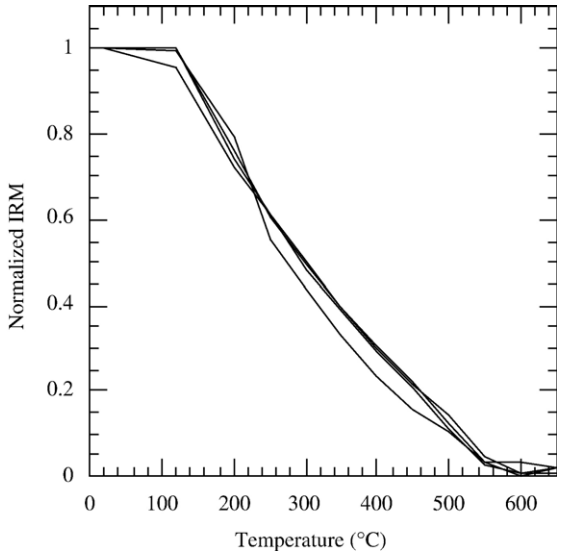

Fig. 6. Stepwise thermal demagnetization of IRMs imparted in a 2.5 T pulse field.

1123 sortable silt mean grain size ($\overline{SS}$) profile lies in the correspondence of MIS 12 at ca. 450 ka, where the $\overline{SS}$ profile shows increased values reflecting stronger near-bottom flow (Hall et al., 2001), while the MD97-2114 ARM/IRM ratios reach a maximum. This difference suggests that the broad coupling between UCDW and MCDW transport was absent during such this interval. This may reflect the severity of the MIS12 glacial interval leading to an extreme northward displacement of the Polar and Subantarctic Fronts which may have either altered the dynamics of the upper levels of the DWBC.

Our data show that (1) the terrigenous sedimentation at site MD97-2114 is under the influence of the upper DWBC and that (2) the dynamics of both upper and middle CDW appear to be modulated by a similar process. Hall et al. (2001) suggest that a pattern of increased glacial production of Antarctic Bottom Water (associated with expanded polar ice sheets), the densest water mass in the open ocean, could be directly responsible for the intensified deep Pacific Ocean inflow over the 1.2 Ma. These authors suggest that the Antarctic Bottom Water production rate might be linked to the magnitude of the Ekman transport driven by winds at the latitude of Drake Passage (Rahmstorf and England, 1997; Toggweiler and Samuels, 1993). Such a process may also impact upon the formation of shallower UCDW, supplied primarily from the eastern South Pacific Ocean and western Indian Ocean (Callahan, 1972; Orsi et al., 1995). Nonetheless, at our shallower site, we cannot discount the possibility that the observed changes in strength of the DWBC might be driven by a direct impingement of an invigorated ACC as a consequence of northward expansion of a stronger westerly wind belt.

5. Conclusions

Core MD97-2114 on the northern flank of the Chatham Rise, preserves a continuous depositional record of sedimentation off eastern New Zealand over the past ca. 1.06 Ma, with an average sediment accumulation rate of ~2.6 cm/kyr. The magnetic and isotope proxies contain evidence for an external forcing mechanism driving the dynamics of the upper CDW component of the DWBC inflow to the Pacific Ocean. On a long-term trend, this flow variability is characterized by varying strengths of the upper CDW component of the DWBC, with two main perturbations centered at 870 ka and 450 ka. This evidence is broadly consistent with those reported from grain-size based paleocurrent analyses of sediment material recovered at Site 1123 under the influence of the middle CDW. The delay between the two main perturbations of the Deep (Pacific) Western Boundary Current, centered at 870 ka and 450 ka, and the mid-Pleistocene transition period (from 920 ka to around 530-540 ka; Schmieder et al., 2000) may manifest a stepwise adaptation and modification of

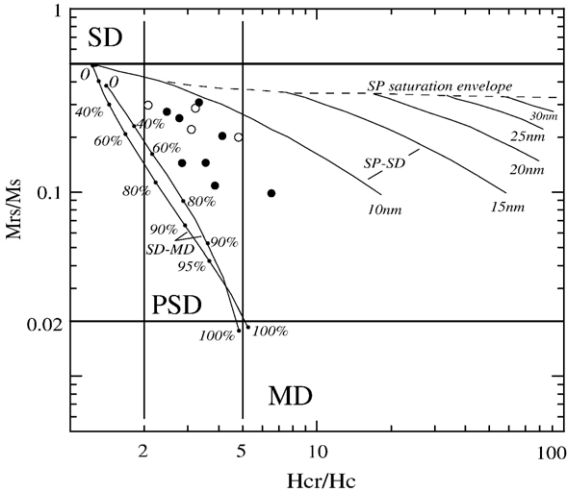

Fig. 7. Mr/Ms and Hcr/Hc data of representative samples from MD97-2114 (solid circles), plotted on the theoretical Day plot curves calculated for magnetite. The remanence and the coercivity ratio of these samples can be interpreted as pseudo-single domain magnetite (PSD; $0.5<d<10$ μm). Only one sample, near the bottom of the sequence (sample MD 18–55 at 25.55 mbsf: Mr/Ms=0.1; Hcr/Hc=6.6), deviates from the standard PSD values, possibly indicating a mixture of PSD and SP (<0.03 μm) magnetite grains (Dunlop, 2002a, b). Tephra layer samples are indicated by open circles. Numbers along curves are volume fractions of the soft component (SP or MD) in mixtures with SD grains (modified from Dunlop, 2002a).

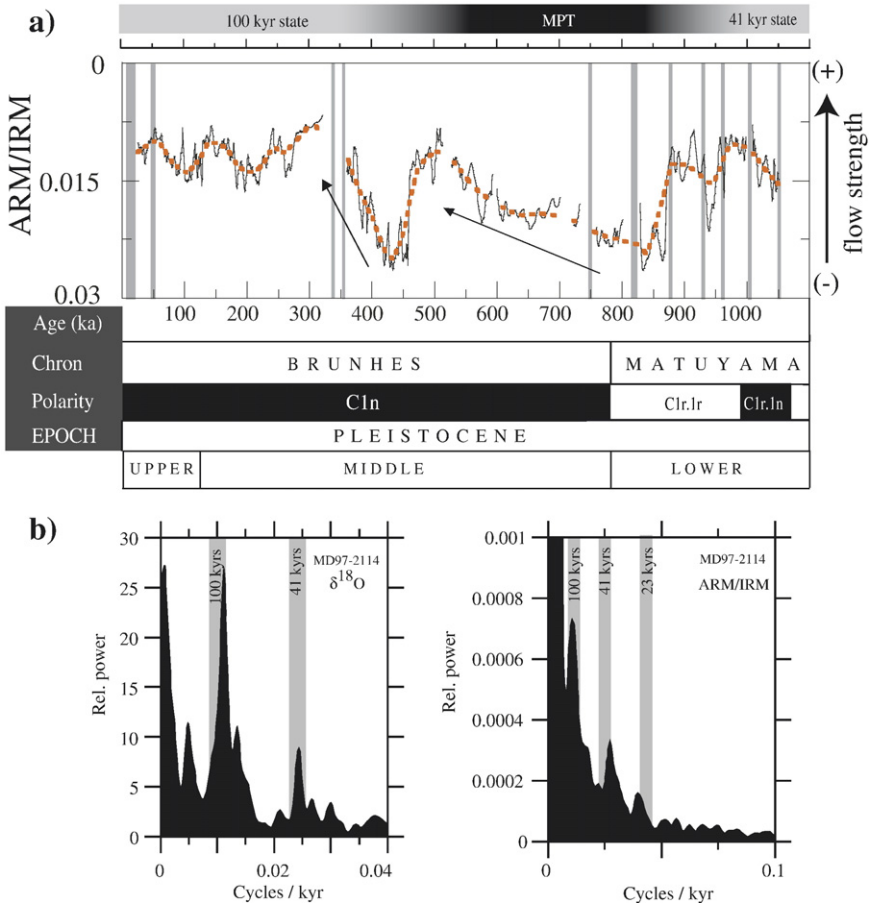

Fig. 8. (a) Grain-size proxy record along MD97-2114. The ARM/IRM data series shows a distinctive long-term trend, which indicates that the strength of this thermohaline inflow was characterized by a switch-like behavior with two main perturbations centered at 870 ka (MIS 22) and 450 ka (MIS 12). Weighted curve fit at 6 % is shown (red line) (Chambers et al., 1983). Vertical bars mark the position of rhyolitic tephra layers. (b) Results of Blackman–Tukey spectral analysis of the $\delta^{18}O$ and ARM/IRM data series sampled at 0.5 kyr intervals, and windowed with a Bartlett taper function producing an averaging bandwidth β. For the ARM/IRM data series: length of the autocov. series 30%; $\beta=0.0047$; error estimation on the power spectrum is $0.546324<\Delta power/Power<2.53694$. For the $\delta^{18}O$ data series: length of the autocov. series 60%; $\beta=0.0024$; error estimation on the power spectrum is $0.451865<\Delta power/Power<4.35793$. The Milankovitch frequencies, with the associated bandwidth β, are highlighted in gray. MPT = mid-Pleistocene transition.

the global thermohaline circulation during this transition of the global climate system. As noted by Schmieder et al. (2000), the mid-Pleistocene transition should not regarded as a gradual transition from a '41 kyr world' to a '100 kyr world', but rather as a third, contrasting state of the global circulation system marked by somewhat weaker deep water exchange.

Acknowledgments

We thank L. Carter and S. Brachfeld who provided constructive comments that helped to improve this manuscript. We are grateful to C. Laj for his help during our visit at the LSCE. K. Verosub, M. Cobianchi, C. Lupi, V. Luciani, G. Villa and T. Naish are thanked for their insightful comments. AV and FF are grateful to the PNRA (Programma Nazionale di Ricerche in Antartide) for financial support. IRH acknowledges the support of the UK Natural Environment Research. We thank the Institut Polaire Francais Paul Emile Victor (IPEV) for technical support and for making the research vessel *Marion Dufresne* available for core retrieval.

References

Blackman, R.B., Tukey, J.W., 1958. The Measurement of Power Spectra from the Point of View of Communication Engineering. Dover Publications, New York.

Callahan, J.E., 1972. The structure and circulation of deep water in the Antarctic. Deep-Sea Res. 19, 563–575.

Cande, S.C., Kent, D.V., 1995. Revised calibration of the geomagnetic polarity timescale for the Late Cretaceous and Cenozoic. J. Geophys. Res. 100, 6093–6095.

Carter, R.M., Carter, L., 1996. The abyssal Bounty Fan and lower Bounty Channel: evolution of a rifted-margin sedimentary system. Mar. Geol. 130, 181–202.

Carter, L., McCave, I.N., 1994. Development of sediment drifts approaching an active plate margin under the SW Pacific Deep Western Boundary Current. Paleoceanography 9, 1061–1085.

Carter, L., Carter, RM., McCave, I.N., Gamble, J., 1996. Regional sediment recycling in the abyssal Southwest Pacific Ocean. Geology 24, 735–738.

Carter, L., Alloway, B., Shane, P., Westgate, J., 2004a. Deep-ocean record of major late Cenozoic rhyolitic eruptions from New Zealand. N. Z. J. Geol. Geophys. 47, 481–500.

Carter, L., Carter, R.M., McCave, I.N., 2004b. Evolution of the sedimentary system beneath the deep Pacific inflow off eastern New Zealand. Mar. Geol. 205, 9–28.

Chambers, J.M., Cleveland, W.S., Kleiner, B., Tukey, P.A., 1983. Graphical Methods for Data Analysis. Duxbury, Boston.

Cobianchi, M., Lupi, C., Luciani, V., Florindo, F., Venuti, A., Zerba, P., 2005. Upper Quaternary bio-magnetostratigraphy from Chatham Rise (SW Pacific Ocean): a framework for paleoceanographic interpretation. Geophys. Res. Abstr. 7, 06474.

Day, R., Fuller, M., Schmidt, V.A., 1977. Hysteresis properties of titanomagnetites: grain size and compositional dependence. Phys. Earth Planet. Inter. 13, 260–267.

Dunlop, D.J., 2002a. Theory and application of the Day plot (Mrs/Ms versus Hcr/Hc): 1. Theoretical curves and tests using titanomagnetite data. J. Geophys. Res. 107 (B3), 2056. doi:10.1029/2001JB000486.

Dunlop, D.J., 2002b. Theory and application of the Day plot (Mrs/Ms versus Hcr/Hc): 2. Application to data for rocks, sediments, and soils. J. Geophys. Res. 107 (B3), 2057. doi:10.1029/2001JB000486.

EPICA Community Members, 2004. Eight glacial cycles from an Antarctic ice core. Nature 429, 623–628.

Hall, I.R., McCave, I.N., Shackleton, N.J., Weedon, G.P., Harris, A.H., 2001. Intensified deep Pacific inflow and ventilation in Pleistocene glacial times. Nature 412, 809–812.

Hall, I.R., Carter, L., Harris, S.E., 2002. Major depositional events under the deep Pacific inflow. Geology 30, 487–490.

Hall, I.R., McCave, I.N., Zahn, R., Carter, L., Knutz, P.C., Weedon, G.P., 2003. Paleocurrent reconstruction of the deep Pacific inflow during the middle Miocene: reflections of East Antarctic Ice Sheet growth. Paleoceanography 18, 1040. doi:10.1029/2002PA000817.

Hesse, P.P., 1994. Evidence for bacterial palaeoecological origin of mineral magnetic cycles in oxic and sub-oxic Tasman Sea sediments. Mar. Geol. 117, 1–17.

Kennett, J.P., 1981. Marine tephrochronology. In: Emiliani, C. (Ed.), The Sea, vol. 7. John Wiley, New York, pp. 1373–1436.

Kissel, C., 2005. Magnetic signature of rapid climatic variations in glacial North Atlantic, a review. Comptes Rendus - Geosci. 337, 908–918.

Lean, C.M.B., McCave, I.N., 1998. Glacial to interglacial mineral magnetic and palaeoceanographic changes at Chatham Rise, SW Pacific Ocean. Earth Planet. Sci. Lett. 163, 247–260.

Lisiecki, L.E., Raymo, M.E., 2005. A Pliocene-Pleistocene stack of 57 globally distributed benthic $\delta^{18}O$ records. Paleoceanography 20, PA1003. doi:10.1029/2004PA001071.

McCave, I.N., Carter, L., 1997. Recent sedimentation beneath the Deep Western Boundary Current off northern New Zealand. Deep-Sea Res., I 44, 1203–1237.

McCave, I.N., Hall, I.R., 2006. Size sorting in marine muds: processes, pitfalls and prospects for palaeoflow-speed proxies. Geochem., Geophys., Geosyst. 10, Q10N05. doi:10.1029/2006GC001284.

Meynadier, L., Valet, J.P., Grousset, F.E., 1995. Magnetic-properties and origin of Upper Quaternary sediments in the Somali Basin, Indian-Ocean. Paleoceanography 10, 459–472.

Mildenhall, D.C., Hollis, C.J., Naish, T.R., 2004. Orbitally-influenced vegetation record of the Mid-Pleistocene Climate Transition, offshore eastern New Zealand (ODP Leg 181, Site 1123). Mar. Geol. 205, 87–111.

Morris, M., Stanton, B., Neil, H., 2001. Subantarctic oceanography around New Zealand: preliminary results from an ongoing survey. N. Z. J. Mar. Freshwater Res. 35, 499–519.

Moskowitz, B.M., Frankkel, R.B., Bazylinski, D.A., 1993. Rock magnetic criteria for detection of biogenetic magnetite. Earth Planet. Sci. Lett. 120, 283–300.

Murphy, R.J., Pinkerton, M.H., Richardson, K.M., Bradford-Grieve, J.M., Boyd, P.W., 2001. Phytoplankton distributions around New Zealand derived from SeaWiFs remotely sensed ocean colour data. N. Z. J. Mar. Freshwater Res. 35, 343–362.

Orsi, A.H., Whitworth, T., Nowlin Jr., W.D., 1995. On the meridional extent and fronts of the Antarctic Circumpolar Current. Deep-Sea Res. 42, 641–673.

Paillard, D., Labeyrie, L., Yiou, P., 1996. Macintosh program performs time-series analysis, Eos Transition. AGU 77, 379.

Press, W.H., Flannery, B.P., Teukolsky, S.A., Vetterling, W.T., 1993. Numerical Recipes. Cambridge University Press, Cambridge.

Rahmstorf, S., England, M.H., 1997. Influence of Southern Hemisphere winds on North Atlantic Deep water flow. J. Phys. Oceanogr. 27, 2040–2054.

Rintoul, S.R., Hughes, C.W., Olbers, D., 2001. The antarctic circumpolar current system. In: Siedler, G., Church, J., Gould, J. (Eds.), Ocean Circulation and Climate: Observing and Modelling the Global Ocean. International Geophysics Series. . International (III), vol. 77. Academic Press, San Diego, pp. 271–302.

Roberts, A.P., Turner, G.M., 1993. Diagenetic formation of ferrimagnetic iron sulfide minerals in rapidly deposited marine-sediments, South-Island, New-Zealand. Earth Planet. Sci. Lett. 115, 257–273.

Rousse, S., Kissel, C., Laj, C., Eiríksson, J., Knudsen, K.-L., 2006. Holocene centennial to millennial-scale climatic variability: Evidence from high-resolution magnetic analyses of the last 10 cal kyr off North Iceland (core MD99-2275). Earth Planet. Sci. Lett. 242, 390–405.

Rowan, C.J., Roberts, A.P., 2006. Magnetite dissolution, diachronous greigite formation, and secondary magnetizations from pyrite oxidation: unravelling complex magnetizations in Neogene marine sediments from New Zealand. Earth Planet. Sci. Lett. 241, 119–137.

Schmieder, F., Von Dobeneck, T., Bleil, U., 2000. The Mid-Pleistocene climate transition as documented in the deep South Atlantic Ocean: initiation, interim state and terminal event. Earth Planet. Sci. Lett. 179, 539–549.

Shackleton, N.J., Berger, A., Peltier, W.R., 1990. An alternative astronomical calibration of the lower Pleistocene timescale based on ODP site 677. Trans. R. Soc. Edinb. Earth Sci. 81, 251–261.

Shipboard Scientific Party, 1999. Site 1123. In: Carter, R.M., McCave, I.N., Richter, C., Carter, L., et al. (Eds.), Proc. ODP, Init. Repts., 181. Texas A&M University, College Station, TX 77845-9547, U.S.A, pp. 1–184 (CD-ROM).

Shipboard Scientific Party, 2001. Site 1167. In: O'Brien, P.E., Cooper, A.K., Richter, C., et al. (Eds.), Proc. ODP, Init. Repts., vol. 188. Ocean Drilling Program, College Station, TX, pp. 1–97. doi10.2973/odp.proc.ir.188.105.2001.

Smale, D., 1990. Distribution and provenance of heavy minerals in the South Island-a review. N. Z. J. Geol. Geophys. 33, 557–571.

Snowball, I., Moros, M., 2003. Saw-tooth pattern of North Atlantic current speed during Dansgaard-Oeschger cycles revealed by the magnetic grain size of Reykjanes Ridge sediments at 59°N. Paleoceanography 18 (2), 1026. doi:10.1029/2001PA000732.

Toggweiler, J.R., Samuels, B., 1993. Is the magnitude of the deep outflow from the Atlantic Ocean actually governed by Southern Hemisphere winds? In: Heimann, H. (Ed.), The Global Carbon Cycle. Springer-Verlag, New York, pp. 333–366.

Warren, B.A., 1973. Transpacific hydrographic sections at latitudes 43°S and 28°S: the SCORPIO Expedition-II deep water. Deep-Sea Res. 20, 9–38.

Warren, B.A., 1981. Deep circulation of the world ocean. In: Warren, B.A., Wunsch, C. (Eds.), Evolution of Physical Oceanography. MIT, Cambridge, MA, pp. 6–41.

Weedon, G.P., 2003. Time-Series Analysis and Cyclostratigraphy: Examining Stratigraphic Records of Environmental Cycles. Cambridge University Press, Cambridge.

Weeks, R., Laj, C., Endignoux, L., Fuller, M., Roberts, A., Manganne, R., Blanchard, E., Goree, W., 1993. Improvements in long-core measurement techniques: applications in palaeomagnetism and palaeoceanography. Geophys. J. Int. 114, 651–662.

Whitworth, T., Warren, B.A., Nowlin, W.D., Rutz, S.B., Pillsbury, R.D., Moore, M.I., 1999. On the deep western-boundary current in the Southwest Pacific Basin. Prog. Oceanogr. 43, 1–54.